

# Language-Native Materials Processing Design by Lightly Structured Text Database and Reasoning Large Language Model

Yuze Liu,<sup>1,3</sup> Zhaoyuan Zhang,<sup>1,3</sup> Xiangsheng Zeng,<sup>2</sup> Yihe Zhang,<sup>2</sup> Leping Yu,<sup>2</sup> Liu Yang,<sup>4</sup> Lejia Wang,<sup>2, 5\*</sup> Xi Yu<sup>1\*</sup>

1. *State Key Laboratory of Advanced Materials for Intelligent Sensing, Key Laboratory of Organic Integrated Circuit, Ministry of Education & Tianjin Key Laboratory of Molecular Optoelectronic Sciences, Department of Chemistry, School of Science, Tianjin University, Tianjin 300072, China*
2. *Boronmatrix Advanced Materials Technology Co., Ltd., No 3938 Wenchuan Road, Baoshan District, Shanghai City, 200949, China*
3. *Language Intelligence Technology Co., Ltd., Haihe Education Park, Jinnan District, Tianjin City, 300350, China*
4. *College of Intelligence and Computing, Tianjin University, Tianjin 300072, China*
5. *School of Materials and Chemical Engineering, Ningbo University of Technology, Ningbo, 315211, China*

\* Authors to whom correspondence should be addressed: [xi.yu@tju.edu.cn](mailto:xi.yu@tju.edu.cn) or [wanglejia@nbut.edu.cn](mailto:wanglejia@nbut.edu.cn)

**Abstract:** Materials synthesis procedures are predominantly documented as narrative text in protocols and lab notebooks, rendering them inaccessible to conventional structured data optimization. This language-native nature poses a critical challenge for complex, multistage processes—such as the preparation of boron nitride nanosheet (BNNS)—where outcomes depend on path-dependent choices in exfoliation and functionalization. Here, we recast synthesis planning as a text reasoning task enabled by a lightly structured text database, which preserves the conditional logic and causal contexts essential for expert-like decision-making. Building on a heterogeneous schema that indexes both narrative excerpts and computable entities (e.g., reaction conditions), our system implements a hybrid retrieval engine to combine semantic context with precise parameter filtering. On top of this, the framework operates in two modes, i.e. retrieval-augmented generation (RAG), which grounds recommendations in retrieved evidence modules, and experience-augmented reasoning (EAR), which uses iteratively refined text guides distilled from multi-source narrative data. Instead of suggesting single “optimal” settings, the system produces interpretable guidance aligned with expert reasoning patterns—hypotheses, parameter ranges, and citation-backed standard operating procedures—that support iterative planning and failure diagnosis. We validated this framework on the targeted exfoliation of BNNS, a process highly sensitive to

multivariate constraints. The system successfully identified optimal combinations of grinding aids, milling configurations, and separation strategies from a wide range of literature-reported methods, which were experimentally verified to yield high-quality nanosheets, illustrating the potential of language-native reasoning to streamline critical operations in materials processing.

## Introduction

While machine learning has revolutionized materials science<sup>1-4</sup> by leveraging structured datasets to predict properties and screen candidates<sup>5-7</sup>, a vast frontier of process development remains inaccessible to these tools<sup>8</sup>. A substantial portion of experimental knowledge—specifically synthesis procedures, contingencies, and troubleshooting heuristics—is "language-native,"<sup>9,10</sup> residing in prose and protocols rather than structured tables. In these narratives, the critical decision signals are encoded in the nuances of order, conditionality, and provenance. Forcing this rich evidence into rigid tabular formats strips away the context required for experimental planning<sup>11</sup>, rendering conventional supervised learning ill-suited for capturing the complexities of practical laboratory work.

The preparation of boron nitride nanosheet (BNNS) serves as a compelling exemplar of this challenge<sup>12,13</sup>. Unlike simple structure-property mappings, BNNS preparation involves a tightly coupled, multistage workflow including pretreatment, milling or sonication processing and post-treatment like centrifuge and dialysis. In the whole process, upstream choices dictate downstream processing windows. Experimentalists must navigate a path-dependent decision space<sup>14</sup>, balancing performance metrics against real-world constraints such as reagent cost, equipment availability, and impurity tolerance. Because these trade-offs and feedback loops are documented almost exclusively in textual literature and lab notes, BNNS preparation constitutes a multifactorial decision problem that requires interpreting procedural logic rather than merely optimizing numerical variables. Addressing this necessitates a system capable of reasoning over textual knowledge in a manner akin to human experts<sup>15</sup>.

Large Language Models (LLMs) offer a promising avenue<sup>16-19</sup> to decipher such language-native evidence, leveraging their inherent capacity to process procedural text. However, current implementations<sup>20-25</sup> in materials science generally treat LLMs as passive extraction tools or simple interfaces for rigid database APIs, leaving their reasoning potential largely untapped. Information extraction pipelines<sup>26-30</sup>, for instance, effectively organize entities into knowledge graphs<sup>31-37</sup> but often flatten procedural nuances — stripping away the dynamic conditionals, feedback loops, and causal links that are essential for decision-making. Similarly, while existing autonomous agents<sup>38,39</sup> excel at protocol execution<sup>40-45</sup> and parameter tuning<sup>46</sup>, they often lack the heuristic reasoning required to deliberate on the qualitative trade-offs inherent in complex synthesis. In contrast, practical synthesis planning resembles clinical decision-making, requiring a system that can reason through dependencies rather than just

retrieve facts<sup>47</sup>. Crucially, the chain-of-thought (CoT) reasoning<sup>48</sup> intrinsic to advanced LLMs naturally encapsulates the conditional logic, path branching, and dynamic procedural elements embedded within these narratives. By treating LLMs as reasoning engines capable of navigating this complexity, we can enable them to emulate expert deliberation—weighing multivariate constraints to guide the flexible, path-dependent decision spaces inherent in materials processing<sup>16</sup>.

In this study, we introduce a Language-Native Materials Processing (LNMP) framework that treats natural-language experimental evidence as a primary data modality for synthesis design. As illustrated in **Fig. 1**, we construct a heterogeneous database constructed from over 3,500 BNNS-related publications with modular LLM prompts (see the Preparation module example in **Fig. 3a**). Full-article content—preparation protocols, characterization results, mechanistic inferences, theoretical modeling, and tabular data—is converted into lightly structured records. Each record comprises evidence-linked modules (actions, materials, instruments, conditions, conditional guards, characterization protocols, theoretical models, and mechanistic reasoning) co-stored with typed fields (e.g., numeric ranges, categorical terms, textual qualifiers) and bidirectional provenance links to the source text. The light structuring defines a stable

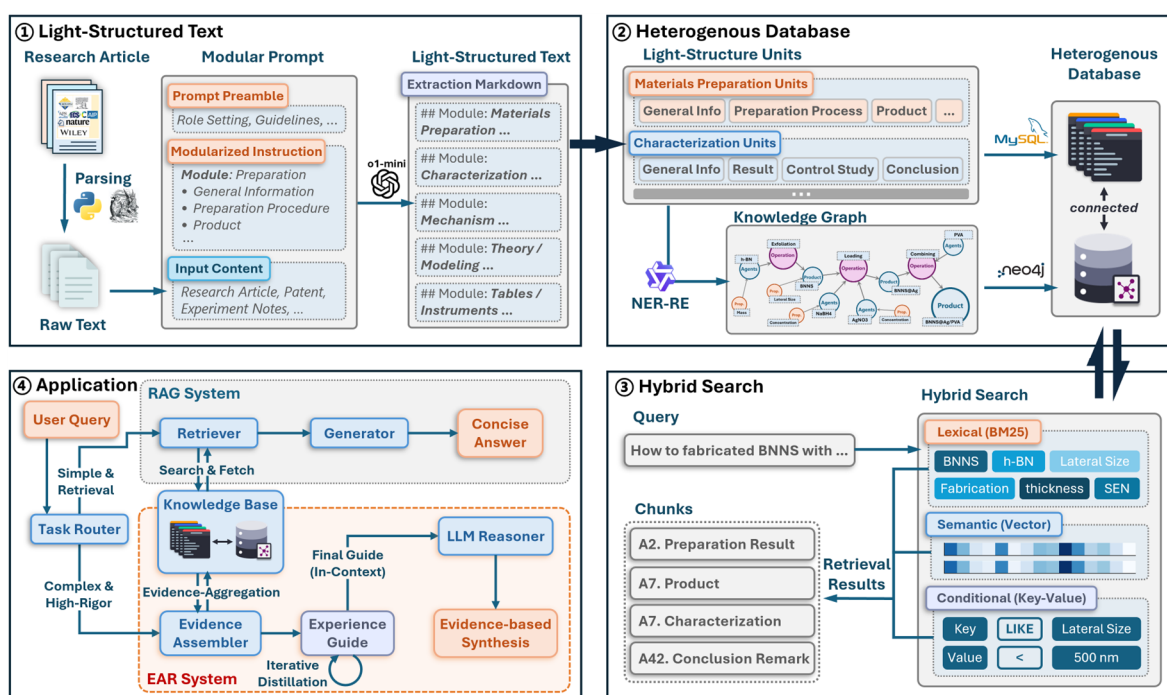


**Figure 1:** Framework of an intelligent AI system driven by a heterogeneous database for BNNS-based thermal conductive materials. (a) Light-structured text with hierarchical topic organization is generated from scientific literature using modular prompting to reconstruct information from unstructured texts. (b) The structured text is decomposed into semantic units, which are then converted into knowledge graphs via named entity recognition and relation extraction (NER-RE), forming a heterogeneous knowledge base. (c) Target text blocks are retrieved through hybrid methods including BM25, dense vector search, and numerical condition filtering. (d) The database is integrated into downstream AI systems such as retrieval-augmented generation (RAG) and structured data extraction pipelines, serving as a domain-specific knowledge repository and retrieval engine.

backbone while preserving rich narratives under higher-level headings (e.g., preparation, characterization, mechanisms, modeling) and retaining verifiable, evidence-linked snippets at the subheading level. Unlike rigid schemas that discard context, we employ LLMs to convert full-article content into lightly structured narrative modules. This architecture establishes a dual-layer backbone: it organizes narrative evidence into distinct semantic modules (e.g., preparation, mechanism) to preserve contextual logic for targeted reasoning, while simultaneously extracting computable entities and relations (NER/KG) to enable precise filtering; representative database entries illustrating the parallel LS, JSON, and KG formats are provided in **Supplementary Data 1**. This design mitigates the fragmentation typical of standard RAG while avoiding the information loss of overly rigid extraction. Consequently, the system supports a hybrid retrieval engine that unifies semantic understanding with lexical precision and explicit parametric constraints (e.g., lateral size < 500 nm).

On top of this database, the reasoning LLM operates in two complementary modes. RAG grounds recommendations in specific, traceable literature evidence. Crucially, we introduce Experience-Augmented Reasoning (EAR), which consults distilled “experience units”—heuristics, failure modes, and laboratory priors iteratively refined from multi-source narratives—to emulate expert heuristics derived from prior experimental outcomes.

We applied this framework to the targeted exfoliation of BNNS, a process governed by sensitive, multivariate constraints. By reasoning over the hybrid database, the system successfully identified optimal combinations of grinding additives, milling configurations (e.g., ball-to-powder ratios), and separation strategies from diverse literature methods. These AI-generated protocols were experimentally verified to yield high-quality BNNS, demonstrating that integrating lightly structured text database with LLM-driven reasoning enables precise, mechanism-guided process optimization that is not readily attainable using numeric-only methods alone.

## **Encoding Materials Knowledge via Lightly Structured Databases**

### **Narrative and Lightly Structured Dataset**

The dataset for BNNS-polymer thermally conductive composites was derived from over 3,500 literature articles identified through a systematic search and screening process (**Table S1**; **Supplementary Note 1**). A modular LLM prompting strategy was then applied to extract and organize the content, generating “lightly structured” narrative data designed to balance machine parsability with the preservation of semantic richness (see Preparation module example in **Fig. 2a**). The prompt templates used for data extraction are provided in **Supplementary Data 2**. Unlike rigid tabular schemas<sup>26</sup>, this format imposes a hierarchical structure: high-level semantic categories (e.g., preparation, characterization, theoretical modeling, mechanism study, and tabular data) form the stable backbone, while lower-level

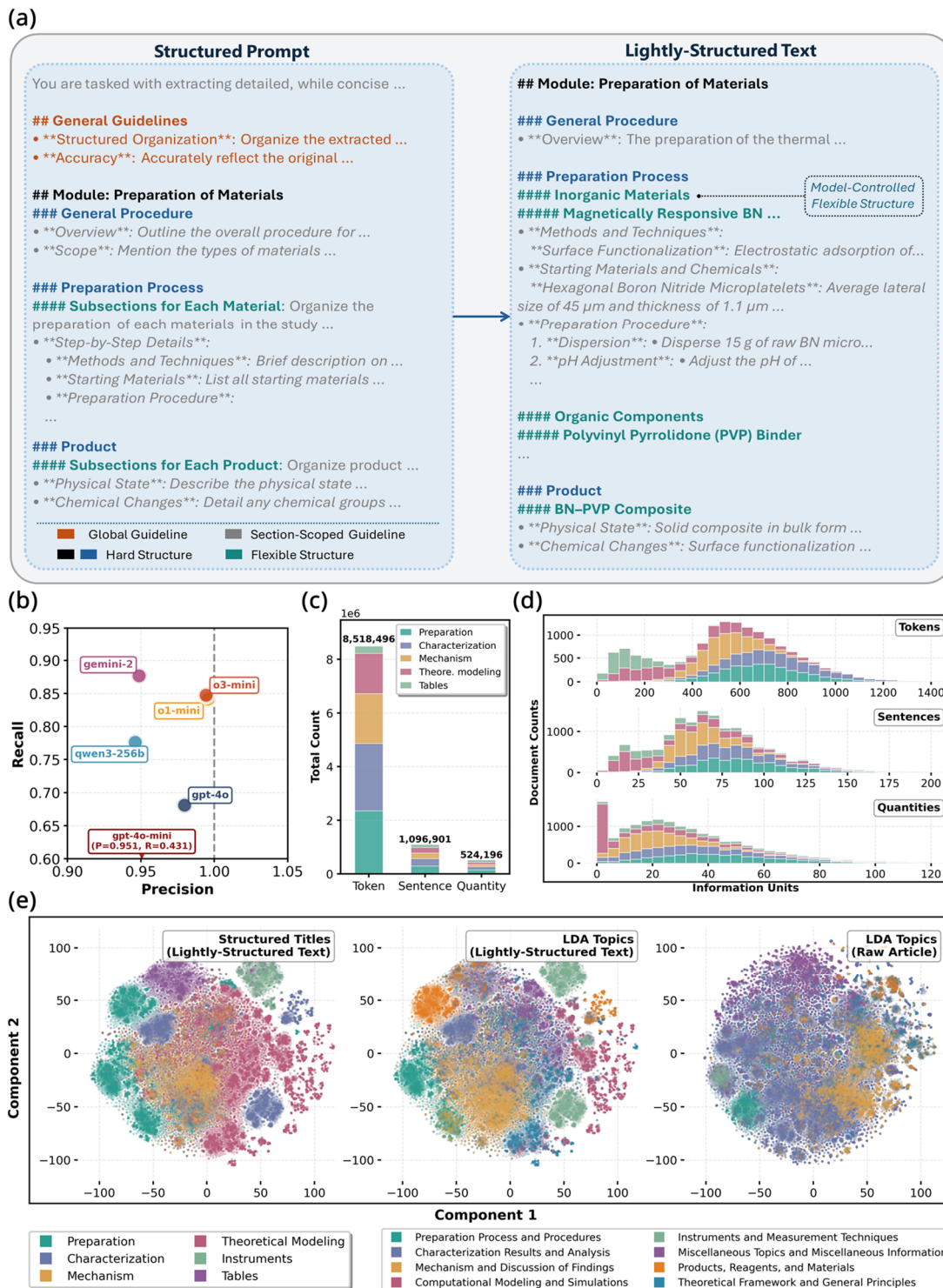


**Figure 2:** Extraction and analysis of lightly structured texts. (a) Illustrates the construction of structured prompts by integrating hard and flexible structural headings, guided by domain-specific knowledge, to enable LLMs to generate lightly structured text. (b) Shows the performance of different large language models in precision and recall when mapping numerical information from 80 sample articles (c-d) Distribution of information units in the extracted lightly structured texts, with (d) illustrating the variation in token, sentence and quantity counts across documents. (e) t-SNE visualization of the lightly structured text, comparing customized title (left 1) with LDA-derived topic (left 2); the strong alignment between title boundaries and topic distributions indicates that the lightly structured title capture coherent semantic module, whereas LDA of original texts (right 1) reveals more topic mixing, highlighting the enhanced focus achieved through reconstruction.

subfields preserve evidence-linked narrative snippets.

This "light-structuring" approach is central to our framework. We initially attempted to extract data into strict, pre-defined schemas. However, this resulted in significant data loss or hallucination due to the mismatch between rigid templates and the highly flexible, irregular descriptions typical of materials literature. By contrast, light structuring achieves two critical goals: (1) Enhanced Organization, it improves content categorization and reduces redundancy compared to raw text, mitigating common RAG challenges such as fragmentation and incoherence.<sup>49-51</sup> (2) Contextual Fidelity, it retains experimental nuances and mechanistic reasoning by allowing flexible narrative entry under structured headers. This ensures that the dataset captures the full provenance of the synthesis process, balancing the orderliness necessary for retrieval with the detail required for reasoning.

We evaluated the fidelity and structure of this dataset through quantitative benchmarks and topological analysis (**Fig. 2b-e**; detailed extraction metrics and compression ratios are shown in **Supplementary Figs. S2-5**). To assess extraction accuracy, we mapped numerical information from 80 sampled articles into light-structured formats using various LLMs (**Fig. 2b**; comparative extraction outputs for all tested models are listed in **Supplementary Data 3**). Reasoning-capable models (e.g., o1-mini, o3-mini) significantly outperformed standard models (e.g., gpt-4o), with o3-mini achieving the highest recall (~0.85) and o1-mini offering a strong balance of precision and recall. Notably, while some models like gemini-2.5 achieved high recall, they exhibited lower precision due to hallucinations—prioritizing structural coherence over factual fidelity by generating plausible but unsupported data to fill schema gaps. This underscores the necessity of reasoning capabilities in correctly interpreting complex relationships within scientific text.

The resulting database scale and distribution are summarized in **Fig. 2c-d**. The corpus comprises ~8.5 million tokens, ~1.0 million sentences, and ~520,000 quantitative values. The content distribution follows a long-tail pattern: while most entries are concise, a significant subset contains extensive details, reflecting the variability of the literature. "Preparation" and "Characterization" modules dominate the volume, capturing the bulk of procedural knowledge, while "Theoretical Modeling" yields fewer but information-dense entries.

Finally, the structural advantage of this approach is visualized via t-SNE<sup>52</sup> and LDA analysis<sup>53</sup> (**Fig. 2e**). Lightly structured titles (left) display coherent semantic grouping, while LDA-derived topics from structured articles form significantly tighter clusters compared to raw text (right). This cluster separation suggests reduced topic mixing and improved semantic focus. Such structural refinement is particularly critical for BNNS processing, which involves diverse and overlapping methodologies (e.g., mechanical exfoliation, CVD, electrospinning), supporting the role of light structuring in organizing complex procedural knowledge.

## Dual-Layer Organization of Narrative and Computable Data

Building upon the extracted lightly structured narratives, we constructed a heterogeneous database schema (**Fig. 3a**). This architecture transforms raw articles into a multi-layered system comprising provenance, narrative, and computable structures, underpinned by robust external indexing.

The schema begins with the Provenance and Narrative Layer. Article metadata (e.g., unique IDs, titles, authors) serves as the anchor. Linked to this are the "lightly structured" modules that organize domain-specific content into semantic categories—such as Preparation (subfields: Process, Product), Characterization (subfields: Instrument, Results), and Theoretical Modeling. This organization preserves the flow of experimental logic while enabling modular retrieval.

Complementing this is the Computable Structure Layer, which refines narratives into machine-readable formats: Named Entity Recognition (NER)<sup>26</sup> data extracts entities with attributes like type, name, value, and unit; Knowledge Graph (KG)<sup>37</sup> nodes represent numbered elements with types, content, and values; and KG edges define relations (e.g., source-target links with types). This structured layer supports conditional filtering, allowing queries with keyword filters (e.g., thickness < 100 nm, time 0.5 h, speed = 500 rpm) to traverse relations and retrieve precise, evidence-linked text data in narrative layer.

To enable scalable retrieval, we implemented a Hybrid Indexing Mechanism. Dense vector indices store semantic embeddings of module content (utilizing BGE-M3 models<sup>54</sup> with FAISS L2 indexing<sup>55</sup>) to capture semantic meaning, while inverted indexes utilize word-level tokenization for lexical (BM25) precision. This combination supports a hybrid search engine that balances the semantic breadth of vector retrieval with the exact-match constraints of keywords and KG parameters<sup>56-58</sup>.

By integrating numerical aggregations from NER with narrative synthesis, this modular architecture not only enhances interoperability but also significantly reduces information redundancy, as validated in subsequent analyses.

## Context-Aware Retrieval for Generative Reasoning

**Fig. 3b** illustrates the end-to-end hybrid retrieval and RAG pipeline built upon the heterogeneous database, enabling context-aware querying and generation. Unlike conventional RAG systems<sup>59,60</sup>, which fragment articles into numerous disjoint chunks, leading to information fragmentation, retrieval failures, and hallucinations in LLM outputs<sup>50,51,61</sup>, our approach leverages the lightly structured database to maintain coherent, compressed representations of article content. This organization—capturing modular sections like Preparation, Characterization, and Mechanism—allows selective retrieval of relevant modules based on query specifics, ensuring narrative completeness while remaining concise and

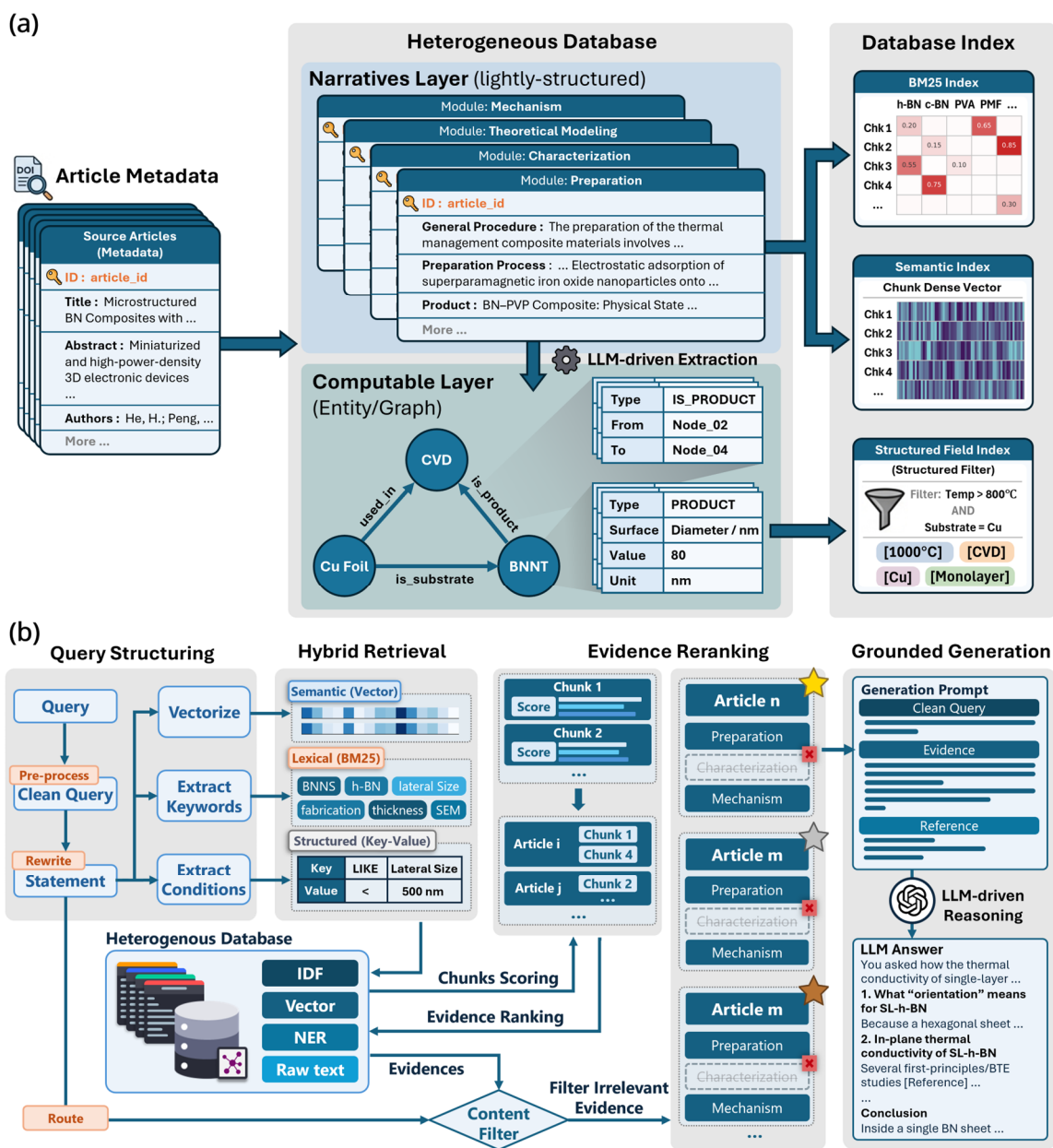


**Figure 3:** Schematic illustration of the heterogeneous database and the RAG architecture. (a) Experimental knowledge is organized into a narrative layer of lightly structured text and a computable layer of structured data. Retrieval is supported by three indices: a lexical index, a BM25-based index, and a structured-field index for constraint-based filtering. (b) The RAG system built on this database operates in four stages: query structuring, hybrid retrieval, evidence re-ranking, and grounded generation, which together transform user queries into factually consistent, evidence-backed outputs.

focused.

Starting from a user query, the system performs query structuring by cleaning, rewriting statements, vectorizing and extracting keywords (e.g., BNNS, thickness, fabrication) and conditional constraints (e.g., key-value filters like lateral size < 500 nm). These elements drive multi-axis retrieval across the database layers: IDF for lexical relevance, vector embeddings for semantic matching, and NER for numerical filtering. Retrieved modules undergo scoring

and ranking, followed by a content filter to select relevant modules (e.g., Preparation, Characterization, Mechanism from articles). Only high-relevance modules proceed, preserving the integrity of empirical narratives without unnecessary dilution. The curated article evidence including references is assembled into a reasoning-aware generation prompt (full RAG prompt templates are provided in **Supplementary Data 4**), along with the clean query, to drive LLM-based reasoning steps, producing verifiable outputs like multi-step SOPs, addressing challenges such as interfacial thermal resistance in BNNS-polymer interfaces.

## **Benchmarking Reasoning Capabilities**

### **Surpassing Conventional Retrieval in Scientific Contexts**

The foundation of our system's efficacy lies in its hybrid retrieval mechanism. As shown in **Fig. 4a**, we evaluated hit rates on a set of 200 domain-specific queries (e.g., targeting specific BNNS dimensions or thermal enhancement mechanisms). Our framework achieved a first-hit success rate of 56.4%, significantly outperforming the baseline RAG's 33.3%, and the cumulative hit rate within the top-12 results increased from 56.4% to 84.6%. Failed hits decreased from 38.5% to 5.1%, indicating robust coverage. **Fig. 4b** plots substantive match hit counts (relevant chunks with high semantic and lexical overlap) as a function of the top-N retrieved results. Our hybrid search (combining 0.6 semantic + 0.3 BM25 + 0.1 KG weights) consistently yields the highest counts, surpassing vector-only and BM25 baselines by up to 40% at N=100; a comprehensive ablation analysis of the hybrid ratios is illustrated in **Supplementary Figs. S6 and S7**. This demonstrates the framework's ability to scale retrieval depth while maintaining relevance, directly supporting the integration of textual description, dependencies, and numerical data for multi-faceted reasoning in composites research.

Building on superior retrieval, the lightly structured data substrate empowers LLMs to generate accurate, quantifiable responses that mimic expert analysis, complete with citations and calculations.

To validate the framework's versatility, we enlisted human experts in BNNS-polymer composite materials studies to curate 60 representative queries spanning five categories: data-retrieval (e.g., extracting specific measurements), recommendation (e.g., suggesting preparation protocols), informational (e.g., explaining mechanisms), integrative summary (e.g., synthesizing trends across studies), and open-ended (e.g., hypothesizing novel composites) tasks. Expert evaluators scored responses on a 1-5 scale for accuracy, completeness, and relevance, comparing our RAG system against: (1) Perplexity (o3 model) with web search capabilities; (2) a standard online model (o3, with external tool-access via OpenAI responses API); and (3) a standard RAG model<sup>60,62</sup> (Chunk Retrieval with o3 model). The complete benchmarking dataset, including the specific queries, model responses, and expert scores rubrics, is provided in **Supplementary Data 5**.

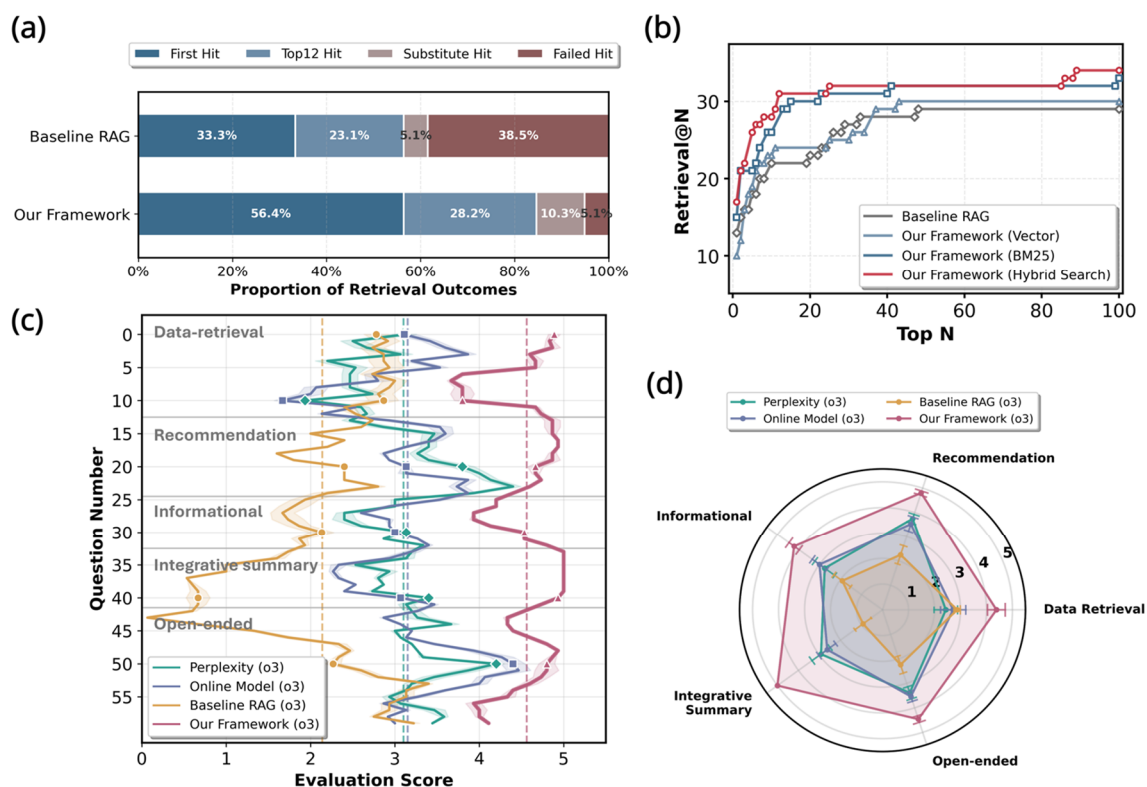


**Figure 4:** Evaluation of retrieval-augmented generation (RAG) performance. (a) Retrieval effectiveness comparison between the baseline RAG system and our proposed framework. (b) Comparison of Retrieval@N across four retrieval strategies: our hybrid framework, keyword-only retrieval, vector-only retrieval, and the baseline RAG system. (c-d) Expert-based manual assessment of 60 domain-specific questions in the BNNS-polymer composites domain, evaluating the factual accuracy and practical utility of generated responses. Methods compared include Perplexity (green), ChatGPT Online (blue), baseline RAG (yellow), and our framework (red), all using o3 as the agentic LLM.

**Fig. 4c** demonstrates the consistent superiority (scores > 4.0) of our framework, particularly in tasks of integrative summaries and recommendations, where aggregating dispersed evidence is essential for multi-hop reasoning. This holistic competence is further captured in **Fig. 4d**, where our system maintains proficiency scores (between 4 and 5) across all axes, clearly outperforming the baselines. While the baseline models (e.g. Perplexity) operated on broader, uncurated search spaces, the superior performance of our framework suggests that domain-specific data curation combined with light-structuring is critical. These results validate the framework's efficacy in reconciling language-native knowledge with computable elements, specifically for material research scenarios dominated by unstructured linguistic data.

### Expert-Level Resolution of Complex Material Queries

To provide a granular understanding beyond the aggregate scores illustrated in **Fig. 4c-d**, we analyze three representative cases that span the spectrum of query complexity—from factual retrieval to expert-level reasoning—as detailed in **Fig. 5**. These cases illustrate how the organization of language-native knowledge critically shapes response quality. For brevity, we compare our framework against Perplexity (o3, web-enabled) and a baseline RAG system that

### Case 1: Precise Retrieval of Research Article Data

**Query:** For an electrospun PVA composite film with a BNNS-to-MWCNT mass ratio of 9:1, how much greater is its thermal conductivity than that of a pure BNNS/PVA film?

**Our System (o3)**

You asked: "(...the user queried question...)"

**## Main Content**  
From Article #2 [TARGET REFERENCE] (...)

Sample	Mass ratio (BNNS:MWCNT)	In-plane thermal conductivity $\lambda$ / ( $W m^{-1} K^{-1}$ )
BNNS/PVA (pure BNNS filler)	10 : 0	9.536
BNNS-MWCNT/PVA	9 : 1	11.49

Absolute increase  $\Delta\lambda = 11.49 - 9.536 \approx 1.95 W m^{-1} K^{-1}$   
Relative (percentage) increase  $(11.49 / 9.536 - 1) \times 100 \% \approx 20.5 \%$

**## Conclusion**  
(...) an absolute gain of about  $2 W m^{-1} K^{-1}$ , corresponding to roughly a 20 % enhancement. (...)

Accurate information acquisition and computation

**Perplexity (o3)**

(...) that uses a BNNS-to-MWCNT mass ratio of 9 : 1 is about  $35.4 W m^{-1} K^{-1}$ . [REFERENCE]  
(...) only BNNSs (no MWCNT bridge) at a comparable 90 wt % BNNS content is  $\approx 70.4 W m^{-1} K^{-1}$ . [REFERENCE]  
 $\Delta TC = 35.4 W m^{-1} K^{-1} - 70.4 W m^{-1} K^{-1} = -35.0 W m^{-1} K^{-1}$   
Relative change =  $-49.7 \%$

Counterfactual Results

**RAG-Chunk (o3)**

- BNNS-only reference (...) ( "BNNSPVA-III" in [REFERENCE]): (...)
- BNNS-MWCNT (...) mass ratio of 9:1 [TARGET REFERENCE]: (...)

Relative gain (percentage):  $(28.7 / 18.63 - 1) \times 100 \% \approx 53 \%$  (...)

Incorrect value extracted from article

### Case 2: Recommendation of Experimental Parameters

**Query:** In the DFT Calculations with Siesta, what is the mesh cutoff value used for the Real-Space Grid?

**Our System (o3)**

Because "mesh-cutoff" is not a universal constant but a user-defined parameter that is tightened or relaxed according to the size of the basis set, the density of valence electrons and the level of accuracy needed, different SIESTA studies adopt different values. (...)

**## Main Content**

Study (system)	Purpose of the calculation	Mesh cut-off chosen	Rationale stated/implicit
Moraes et al. 2012 (...)	Band-structure tuning	150 Ry ( $\approx 2040 eV$ )	"sufficient for accurate real-space grid integration"

(...)

**### How to choose an appropriate mesh-cutoff in SIESTA**

- Convergence target: decide an acceptable change in total energy/force (e.g.  $\leq 1 meV/atom, \leq 0.01 eV \text{ \AA}^{-1}$ ).
- Start from a moderate value ( $\approx 150 Ry$  for s-p systems) and increase until energy, stress and forces stabilize.

(...)

**## Conclusion**  
(...) In the supplied literature the real-space grid cut-off spans from 150 Ry to 800 Ry (and even  $\sim 300 Ry$  in eV units) depending on the accuracy demanded by the property of interest. (...)

Reasoning Chain: Query constraints  $\rightarrow$  Evidence gathering  $\rightarrow$  Rule induction  $\rightarrow$  Conclusion

**Perplexity (o3)**

In the Siesta input file the real-space grid is fixed through the keyword:  
"MeshCutoff 100 Ry"  
Thus the requested mesh-cutoff (i.e., the energy equivalent that determines the grid density) is 100 Rydberg; when the run starts Siesta converts this into the closest FFT-friendly value and reports:  
"InitMesh: Mesh cutoff (required, used) = 100.000 101.039 Ry"  
so the grid actually employed is  $\approx 101 Ry$ . [SIESTA DOCS]

RAG-Chunk (o3)

(...)  
The SIESTA calculations were carried out with a real-space grid "mesh-cutoff" (energy mesh) of 225 Ry [REFERENCE]

Both with erroneous query understanding

### Case 3: Comprehensive Information Acquisition

**Query:** What is the prerequisite for achieving 'dual-alignment' using a dynamic magnetic field in the 3D printing process?

**Our System (o3)**

Here "dual-alignment" refers to the sequential combination of (...). The technique is best illustrated by Chen et al. ("Sequential Dual Alignments...", Adv. Mater., 2024) who used a rotating magnetic field (RMF) after extrusion to obtain highly planar mhBN platelets. [TARGET REFERENCE]

**## Main Content**

### 1. Conceptual background  
Dual-alignment works only if two alignment steps can act on the \*same\* population of fillers without interfering with, or canceling, each other: (...)

### 2. Practical prerequisites  
The requirements fall into four inter-locking categories:  
| Category | Prerequisite | Why it is needed | Typical ranges / remarks |  
<... table content ...>

### 3. Common failure modes if prerequisites are not met  
| Failure symptom | Likely missing prerequisite | Corrective action |  
<... table content ...>

### 4. Parameter guideline (from Chen et al. unless noted)  
- mhBN particle:  $10 \mu m \times 0.3 \mu m$ ,  $Fe_3O_4$  0.2 vol %. (...)

### 5. Cross-validation from related studies  
• Itaoka et al. demonstrated that without magnetic coating, fields  $>10 T$  are required—highlighting why  $Fe_3O_4$  functionalization is essential for practical RMF dual-alignment. [REFERENCE 7]  
(...)

**## Conclusion**  
To realize dual-alignment during 3-D printing with a dynamic magnetic field you need: (...)

Reasoning Chain: Query constraints  $\rightarrow$  Theory analysis  $\rightarrow$  Counterfactual reasoning  $\rightarrow$  Comparison  $\rightarrow$  Conclusion

**Perplexity (o3)**

Achieving "dual-alignment" (i.e., being able to re-orient anisotropic fillers in two orthogonal directions during a single print run) requires that the suspended particles can rotate fast enough to follow the time-varying field. The prerequisite is therefore that the ink's viscosity be low enough that magnetic torque dominates viscous drag so the particles reach the imposed orientation within the short time (sub-second) available between extrusion and solidification [REFERENCE]

Not enough evidence supported

**RAG-Chunk (o3)**

The method relies on applying a time-varying (dynamic) magnetic field several times during the fabrication of a single layer. (...)  
(...) every slice of the CAD model has to be "pre-segmented" into zones that share the same target orientation of the magnetically functionalised fillers.  
In other words, the prerequisite for obtaining the so-called dual-alignment (different orientations in different parts of the same layer and between successive layers) is:  
"First, elements within each print layer must be separated into groups according to their desired orientation." [REFERENCE]

Incorrect Mechanism: The mechanism shown is multi-directional orientation, not dual-alignment

**Figure 5.** Question-answering performance of a language-native heterogeneous knowledge base across three tasks of increasing complexity: (i) a factual query, (ii) multi-step reasoning with rule induction, and (iii) counterfactual analysis of failure modes. Baselines—perplexity-based retrieval and web-augmented ChatGPT—suffer from misinterpretation, incorrect citations, factual hallucinations, and shallow reasoning. In contrast, our system accurately retrieves relevant literature, extracts precise evidence, and demonstrates advanced scientific reasoning, including induction (Case 2) and structured counterfactuals (Case 3).

employs conventional chunk-based document segmentation; all other components (retriever, generator, prompt template) are held constant. Full query-response transcripts and additional analyses for these and other categories are provided in **Supplementary Note 2** and **Supplementary Data 5**.

**Case 1 (Data Retrieval):** The query requests a precise thermal conductivity value under specific experimental conditions. Our system retrieves the relevant study, correctly identifies the matching data point, and performs a simple arithmetic operation to yield an accurate answer. In contrast, Perplexity fails to locate the pertinent source and instead combines values from two unrelated papers, producing a factually incorrect result. The baseline RAG retrieves the correct document but extracts an erroneous numerical value due to fragmentation: the target measurement is split across multiple chunks, disrupting contextual coherence and leading to misinterpretation.

**Case 2 (Recommendation):** The query seeks a recommended mesh cutoff for real space grid calculations in interfacial thermal modeling—a parameter requiring contextual understanding of system scale and computational trade-offs. Our system synthesizes multiple literature examples, categorizes them by material system, and infers general design principles to justify its recommendation. Both Perplexity and the baseline RAG, however, default to replicating the parameter from a single highly ranked paper without adaptation or rationale, offering a non-transferable and thus non-actionable suggestion.

**Case 3 (Mechanistic Reasoning):** The query asks for an explanation of the “dual-alignment” mechanism and its prerequisite conditions. Our framework identifies the seminal paper on dual-alignment alongside supporting studies, reconstructs the authors’ causal reasoning, and extends the analysis by hypothesizing failure modes under violated assumptions—effectively simulating experimental pre-validation. The baseline RAG, by contrast, conflates this concept with “multi-directional orientation” from a 3D printing context, misattributing the underlying physics and delivering a conceptually incoherent summary.

These cases underscore a critical insight that when all pipeline components except knowledge organization are controlled, the lightly structured representation of language-native knowledge—where each module encapsulates the full scope from general context to technical detail to conclusion—preserves the original narrative flow. This contextual integrity ensures that the reasoning chains required for multi-hop inference<sup>63</sup> remain intact, whereas chunk-based evidence, though retrievable, is inherently fragmented and short-range, often severing the very reasoning chains that domain experts rely on. This structural fidelity is what empowers our system to deliver not just accurate facts, but verifiable, expert-aligned guidance across the full range of BNNS fields inquiry.

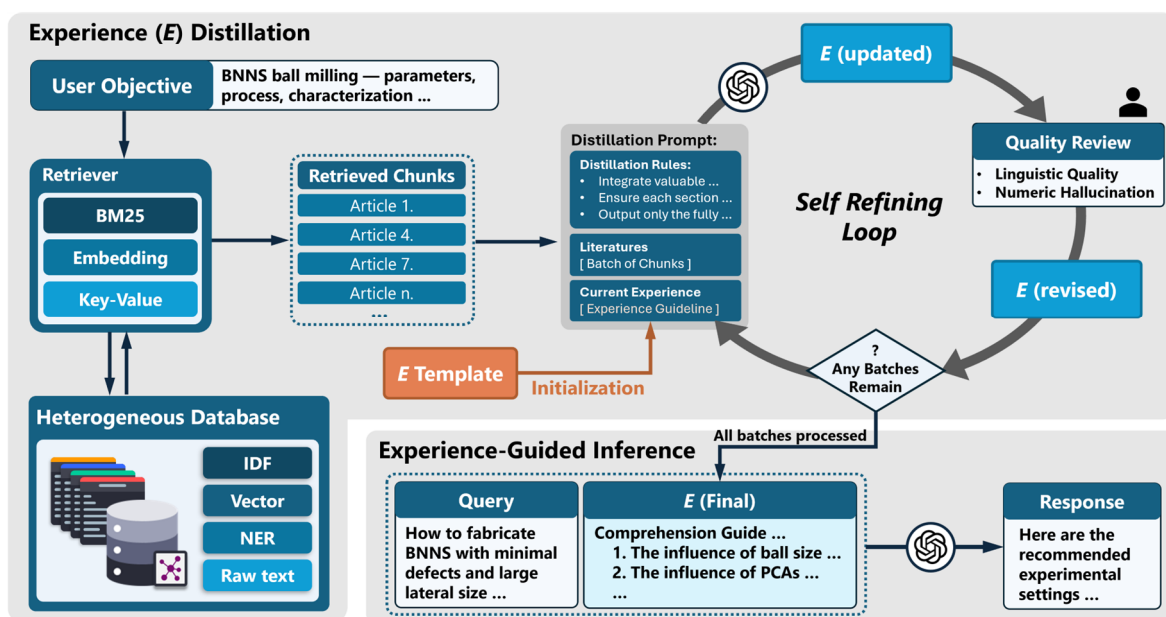


**Figure 6:** Schematic of the experience-augmented reasoning system architecture. A user objective is first defined, which guides the retrieval of relevant information from heterogeneous databases. The retrieved results are then processed through an iterative LLM-driven enhancement loop consisting of: (i) experience summarization and integration by the LLM; (ii) quality assessment and hallucination analysis; (iii) refinement and re-integration of experiences; and (iv) iteration back to step 1. or finalization of an enhanced knowledge base, which serves as an experience context for LLM inference.

## Closed-Loop Optimization of BNNs Synthesis

### The Experience-Augmented Iterative Protocol

Extending the framework's capabilities beyond RAG, we demonstrate its potential for iterative, experience-guided optimization in experimental design, leveraging the heterogeneous database to integrate empirical narratives. This addresses the trial and error nature of materials research by enabling LLMs to refine protocols dynamically, drawing on preserved linguistic descriptions of mechanisms and prior outcomes<sup>39,43</sup>. In a concrete example, retrieval from the database yields lightly structured data from over 200 articles on BNNs preparation by ball milling, which undergoes iterative experience updates to composite a comprehensive guide that serves as an external reference for LLMs, aiding in the design of materials preparation processes.

Starting from a user objective (e.g., “BNNs ball milling—parameters, process, characterization”), the system queries the heterogeneous database and feeds retrieved modules into an iterative loop. An experience (E) template is initialized by summarization and distillation, followed by prompt-guided evolution (see **Supplementary Data 6** for experience-update protocols), batch integration of new chunks, and optional human-in-the-loop quality control (entity checks, hallucination screening). This process refines the experience base into an enhanced context that is then supplied to the LLM, which produces coherent, literature-

grounded guides rather than operating on fragmented RAG chunks.

### **Experimental Realization of Controlled Exfoliation**

To validate the framework in a realistic R&D scenario, we conducted a case study commissioned by a lithium battery manufacturer (facilitated by Shanghai Boronmatrix) targeting BNNS fillers for gel electrolytes. This application imposes stringent and partly conflicting specifications: the nanosheets must be ultrathin (<20 nm) with controlled lateral dimensions, high specific surface area for ion transport, and functional groups (e.g., hydroxyl) for salt dissociation and dispersion, all under tight purity constraints. This presents a quintessential challenge in nanomaterial synthesis, i.e. navigating a vast parameter space populated by disparate literature reports. While numerous exfoliation methods exist, direct replication often fails due to subtle, unrecorded variations in experimental conditions (e.g., specific ball mill energy input, vessel geometry). Consequently, the primary hurdle is not merely identifying a method, but rapidly adapting and iterating literature protocols to function reliably under specific local constraints. We utilized this scenario to demonstrate the framework's unique advantage in accelerating this process.

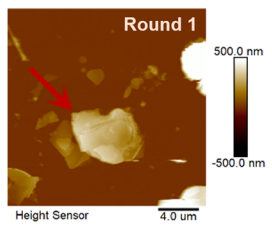
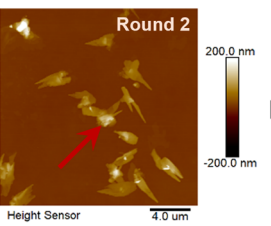
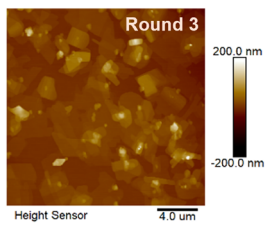
Guided by the "Experience Guideline", the LLM (o3 pro) orchestrated a three-stage iterative optimization for BNNS exfoliation. The final evolved "Experience Guideline" is presented in **Supplementary Data 6**. Instead of acting as a static retrieval system, the model functioned as a reasoning agent, which analyzed feedback from each trial, cross-referenced outcomes with the Experience, and dynamically adjusted the experimental hypothesis. **Table 1** (and **Supplementary Table S3** for comprehensive parameter sets) details the decision, contrasting the specific parameters with the model's strategic rationale at each stage.

**Round 1: Exploration.** The LLM initially proposed a prudent, decoupled strategy, which is mechanical exfoliation in an IPA/water system followed by a separate urea functionalization step. It reasoned that decoupling would maximize controllability and allow intermediate characterization. To counteract the low viscosity of the IPA/water solvent, the LLM proactively introduced 1 wt% PVP to enhance shear stress. However, experimental feedback revealed suboptimal results. The product averaged ~200 nm in thickness (mostly thick flakes) with noticeable media wear and persistent PVP residues.

**Round 2: Mechanism Pivot (Impact -> Shear).** Diagnosing the failure as "impact-induced fracture" due to low solvent viscosity, the LLM pivoted to a viscous shear-dominated regime. It integrated the previously secondary urea functionalization step into a single-step urea-paste milling strategy. High viscosity of the paste would effectively transmit shear forces for exfoliation. To operationalize this shift, the system reconfigured the media to a shear-dense assembly (5/2/1 mm balls with 100:1 BMR).

**Round 3: Refinement.** While Round 2 significantly reduced thickness to ~40 nm, feedback

**Table 1:** Path of LLM-Driven decision making and reasoning across iterative experiments for Case: “Ball Milling Design for BNNS Gel Electrolyte Fillers”

Strategy		Round 1: Exploration	Round 2: Mechanism Pivot	Round 3: Refinement
		Conservative Decoupling	Aggressive Shear Activation	Constraint Optimization
LLM Reasoning	Critical Reflection	<b>Diagnosis (from literature)</b> <b>Limitations:</b> High-energy one-pot methods risk lateral fracture; Organic solvents (e.g., NMP) pose removal/toxicity challenges.	<b>Diagnosis (of Round 1)</b> <b>Inefficient Exfoliation.</b> Low-viscosity solvent <b>avored brittle impact over shear</b> , resulting in thick flakes (>200 nm).	<b>Diagnosis (of Round 2)</b> <b>Media Instability.</b> 5mm balls <b>caused severe ZrO2 bead fracture</b> (contamination); PVP <b>proved difficult to remove</b> .
	Current Decision	<b>Logic: Separating variables</b> • LLM chose a Two-Step process to <b>isolate physical exfoliation</b> from chemical functionalization. • Because IPA/Water (Step 1) has <b>low viscosity</b> , PVP was added effectively as a <b>rheological modifier</b> to enable shear.	<b>Logic: Mechanism shifted</b> • LLM pivoted to One-Step paste milling to utilize <b>Urea's intrinsic viscosity</b> enabling shear. • To increase shear sites, Ball Size was reduced (10/2 → 5/2/1). To <b>compensate for the kinetic energy</b> loss of smaller balls, the BMR was spiked to 100:1.	<b>Logic: Simplify &amp; Optimize</b> • LLM identified that the Urea paste (from Round 2) <b>offers sufficient viscosity</b> , making PVP redundant. • To solve "Bead Fracture", 5mm balls were removed, trusting the high-density Micro-Beads (2/1) to exfoliate via pure shear <b>without high-impact damage</b> .
Experimental Parameters	Process	<b>Two-Step Approach</b> (Separated for control)	<b>One-Step Viscous Milling</b> (Merged for efficiency)	<b>One-Step Viscous Milling</b> (Retained mechanism)
	Media	<b>Large Mix (10/2 mm)</b> BMR 40: 1 (Large balls provide impact energy)	<b>Aggressive Mix (5/2/1 mm)</b> BMR 100 : 1 ↑ (reduce ball size to increase shear)	<b>Micro-Media (2/1 mm)</b> BMR 80: 1 ↓ (avoid high impact by remove large ball)
	Additives	<b>IPA/Water + 1wt% PVP</b> (PVP essential for viscosity)	<b>Urea Paste + Reduced PVP</b> (PVP role diminishing)	<b>Pure Urea Paste (PVP-free)</b> (PVP removed as impurity)
Outcomes	Results	• Thickness: <b>200~300 nm</b> • Lateral Size: $1.49 \pm 0.82 \mu\text{m}$ • Defect: <b>PVP residue</b> <b>Bead Fracture</b>	• Thickness: <b>40~60 nm</b> • Lateral Size: $0.94 \pm 0.45 \mu\text{m}$ • Defect: <b>PVP residue</b> <b>Severe Bead Fracture</b>	• Thickness: <b>7~12 nm</b> ↓ • Lateral Size: $0.85 \pm 0.47 \mu\text{m}$ • Defect: <b>Non-contamination</b>
	AFM Morphology			

indicated minor bead wear and residual organic contamination from the reduced PVP. Integrating these constraints, the LLM executed a final optimization which eliminated PVP (identifying the urea paste itself as sufficiently viscous for stabilization) and refined the media to a 2 mm/1 mm micro-bead combination. This adjustment aimed to maximize shear density while keeping impact energy strictly below the ceramic breakdown threshold.

**Outcome and Efficiency Analysis:** This reasoning chain culminated in a protocol yielding BNNS with an average thickness of ~10 nm—a >90% reduction compared to the initial trial (experimental characterization results are provided in **Supplementary Figs. S8-S13**). While the "urea-paste" methodology draws upon the seminal work of Wu et al.<sup>64</sup>, its deployment here represents a reasoning-driven adaptation rather than simple retrieval. The agent selected this specific strategy from hundreds of candidates only after synthesizing vast literature against the specific failure modes (impact-induced fracture) observed in Round 1. Crucially, the experimentally finalized parameters—specifically the ball-to-material ratio and the multi-scale media combination—diverge significantly from Liu’s original report, reflecting an autonomous

optimization for local equipment constraints.

It is crucial to underscore that this entire decision trajectory—from strategy selection to parameter refinement—was executed autonomously by the system, independent of human intervention. This capability was vividly illustrated during Round 2, where a notable divergence occurred between human expert intuition and the agent's logic. While human researchers tentatively proposed using viscous polymer solutions (e.g., sucrose) as grinding aids, the system critically evaluated and rejected this approach. It cited multi-faceted risks often overlooked in initial screening where the generation of cavitation bubbles impeding shear transfer, heat accumulation difficulties in high-viscosity milling, and, most critically, the industrial non-viability of the requisite post-treatment (time-consuming dialysis). By prioritizing the urea-paste route—which allows for efficient water-washing purification—the system demonstrated a comprehensive foresight that transcended immediate technical feasibility to encompass downstream processability and scalability, effectively correcting the bias of human experts.

In traditional materials R&D, navigating this path—from literature screening and method selection to the granular tuning of kinetic conditions—typically consumes months of labor and involves over a dozen trial-and-error iterations. Our framework reduced the optimization process to three focused experimental rounds within one week under the specified laboratory conditions, demonstrating that the system utilizes "Experience" not merely as a static database, but as a dynamic engine for causal reasoning and process acceleration.

## **Conclusion and Perspective**

This work reconceptualizes materials preparation—exemplified by BNNS—as a text reasoning task, shifting the focus from searching for fixed numeric optima to navigating a decision-making process driven by linguistic logic. We demonstrate that when LLMs are grounded in a "lightly structured" database—one that preserves narrative nuance while exposing computable entities—they can transcend simple information retrieval to perform expert-level experimental design. By integrating EAR with standard retrieval, our framework successfully reconciles literature evidence with accumulated domain heuristics. Crucially, we validated this framework experimentally through the iterative preparation of BNNS. Functioning as a fully autonomous agent, the system demonstrated decision-making capabilities that surpassed human expert intuition—effectively bypassing suboptimal heuristics that often entrap researchers to locate robust global optima. This accelerated reasoning process yielded ultrathin nanosheets (~10 nm) meeting strict specifications in just three iterations, compressing a development cycle that typically spans months of expert trial-and-error.

Furthermore, this framework bridges the gap between linguistic logic and numerical precision, resolving the limitations of traditional machine learning (ML) in unstructured experimental

design<sup>65-67</sup>. Unlike conventional models restricted to fixed parameter spaces, our system orchestrates a symbiotic workflow: the LLM employs qualitative reasoning to navigate the complex "strategy space"—determining routes and mechanisms—before defining structured sub-problems for ML-driven parameter refinement. This fusion acts as a semantic interface that grounds rigorous physical models within heuristic-driven realities, effectively uniting symbolic logic with quantitative precision.

Most significantly, this work constructs the cognitive architecture for future AI agents, addressing their primary technical bottleneck: the lack of structured, domain-specific memory. Current agents often fail in complex tasks due to the absence of a 'world model' to ground their logic. By serving as this robust semantic grounding, our framework empowers LLMs to perform active 'System 2' reasoning—long-horizon planning and dynamic correction—rather than passive retrieval. The BNNS experiment has unequivocally validated the system's efficacy as a central decision-making hub. With this 'reasoning brain' established, the subsequent integration of automated execution and characterization modules will naturally complete the transition to fully closed-loop, autonomous laboratories.

Finally, we would like to emphasize the imperative of constructing 'lightly structured' text databases that balance retrievability with the preservation of rich procedural logic. Just as structured numerical datasets catalyzed the machine learning revolution in materials science, we posit that these text-based substrates—serving as the memory and reasoning foundation for autonomous agents—represent a complementary and equally transformative paradigm. By serving as the interface between human-readable knowledge and machine-usable logic, such infrastructure may stand as the bedrock of next-generation, AI-native materials research.

## Acknowledgement

This work was supported by the Fundamental and Interdisciplinary Disciplines Breakthrough Plan of the Ministry of Education of China (JYB2025XDXM410), Natural Science Foundation of China (Grant No. 22573072, 62476194, U23B2049), and "the Fundamental Research Funds for the Central Universities."

## Reference

1. Butler, K.T., Davies, D.W., Cartwright, H. et al. Machine learning for molecular and materials science. *Nature* **559**, 547-555 (2018). <https://doi.org/10.1038/s41586-018-0337-2>
2. Himanen, L., Geurts, A., Foster, A.S. et al. Data-Driven Materials Science: Status, Challenges, and Perspectives. *Adv. Sci.* **6**, 1900808 (2019). <https://doi.org/10.1002/advs.201900808>

3. Schmidt, J., Marques, M.R.G., Botti, S. et al. Recent advances and applications of machine learning in solid-state materials science. *npj Comput. Mater.* **5**, 83 (2019). <https://doi.org/10.1038/s41524-019-0221-0>
4. Choudhary, K., DeCost, B., Chen, C. et al. Recent advances and applications of deep learning methods in materials science. *npj Comput Mater* **8**, 59 (2022). <https://doi.org/10.1038/s41524-022-00734-6>
5. Sanchez-Lengeling, B., Aspuru-Guzik, A. Inverse molecular design using machine learning: Generative models for matter engineering. *Science* **361**, 360-365 (2018). <https://doi.org/10.1126/science.aat2663>
6. Xie, T. & Grossman, J. C. Crystal graph convolutional neural networks for an accurate and interpretable prediction of material properties. *Phys. Rev. Lett.* **120**, 145301 (2018). <https://doi.org/10.1103/PhysRevLett.120.145301>
7. Bai, X., Li, Y., Xie, Y. et al. High-throughput screening of CO<sub>2</sub> cycloaddition MOF catalyst with an explainable machine learning model. *Green Energy Environ.* **10**, 132-138 (2025). <https://doi.org/10.1016/j.gee.2024.01.010>
8. Olivetti, E. A., Cole, J. M., Kim, E., et al. Data-driven materials research enabled by natural language processing and information extraction. *Appl. Phys. Rev.* **7**, 041313 (2020). <https://doi.org/10.1063/5.0021106>
9. White, A.D. The future of chemistry is language. *Nat. Rev. Chem.* **7**, 457-458 (2023). <https://doi.org/10.1038/s41570-023-00502-0>
10. Tshitoyan, V., Dagdelen, J., Weston, L. et al. Unsupervised word embeddings capture latent knowledge from materials science literature. *Nature* **571**, 95-98 (2019). <https://doi.org/10.1038/s41586-019-1335-8>
11. Yuan, W., Chen, G., Wang, Z. et al. Empowering Generalist Material Intelligence with Large Language Models (Adv. Mater. 32/2025). *Adv. Mater.* **37**: e70084. (2025), <https://doi.org/10.1002/adma.70084>
12. Rasul, M.G., Kiziltas, A., Arfaei, B. et al. 2D boron nitride nanosheets for polymer composite materials. *npj 2D Mater. Appl.* **5**, 56 (2021). <https://doi.org/10.1038/s41699-021-00231-2>
13. Guerra, V., Wan, C., McNally, T. Thermal conductivity of 2D nano-structured boron nitride (BN) and its composites with polymers. *Progress in Materials Science.* **100**, 170-186 (2019). <https://doi.org/10.1016/j.pmatsci.2018.10.002>
14. Wu, W., Zheng, M., Lu, K. et al. Thermally Conductive Composites Based on Hexagonal Boron Nitride Nanosheets for Thermal Management: Fundamentals to Applications. *Composites Part A: Applied Science and Manufacturing.* **169** (March), 107533 (2023). <https://doi.org/10.1016/j.compositesa.2023.107533>

15. Hippalgaonkar, K., Li, Q., Wang, X. *et al.* Knowledge-integrated machine learning for materials: lessons from gaming and robotics. *Nat Rev Mater* **8**, 241-260 (2023). <https://doi.org/10.1038/s41578-022-00513-1>
16. Truhn, D., Reis-Filho, J.S. & Kather, J.N. Large language models should be used as scientific reasoning engines, not knowledge databases. *Nat Med* **29**, 2983-2984 (2023). <https://doi.org/10.1038/s41591-023-02594-z>
17. OpenAI. OpenAI o1 System Card. *OpenAI* (2024). <https://openai.com/index/openai-o1-system-card/>
18. Zheng, Z., Rampal, N., Inizan, T.J. *et al.* Large language models for reticular chemistry. *Nat Rev Mater* **10**, 369-381 (2025). <https://doi.org/10.1038/s41578-025-00772-8>
19. Jablonka, K.M., Schwaller, P., Ortega-Guerrero, A. *et al.* Leveraging large language models for predictive chemistry. *Nat Mach Intell* **6**, 161-169 (2024). <https://doi.org/10.1038/s42256-023-00788-1>
20. Jablonka, K. M., Ai, Q., Al-Feghali, A. *et al.* 14 examples of how LLMs can transform materials science and chemistry: a reflection on a large language model hackathon. *Digital Discovery* **2**, 1233-1250 (2023). <https://doi.org/10.1039/D3DD00113J>
21. Zimmermann, Y., Bazgir, A., Al-Feghali, A. *et al.* 34 Examples of LLM Applications in Materials Science and Chemistry: Towards Automation, Assistants, Agents, and Accelerated Scientific Discovery. arXiv:2505.03049 (2025). <https://arxiv.org/abs/2505.03049>
22. Kang, Y., Lee, W., Bae, T. *et al.* Harnessing Large Language Models to Collect and Analyze Metal-Organic Framework Property Data Set. *J. Am. Chem. Soc.* **147**, 3943-3958 (2025). <https://doi.org/10.1021/jacs.4c11085>
23. Zheng, Z., Zhang, O., Borgs, C. *et al.* ChatGPT Chemistry Assistant for Text Mining and the Prediction of MOF Synthesis. *J. Am. Chem. Soc.* **145**, 18048- 18062 (2023). <https://doi.org/10.1021/jacs.3c05819>
24. Kang, Y., Kim, J. ChatMOF: an artificial intelligence system for predicting and generating metal-organic frameworks using large language models. *Nat Commun* **15**, 4705 (2024). <https://doi.org/10.1038/s41467-024-48998-4>
25. Leng, Y., Zhong, Y., Gu, Z. *et al.* Intelligent, personalized scientific assistant via large language models for solid-state battery research. *ACS Materials Lett.* **7**, 1807-1816 (2025). <https://doi.org/10.1021/acsmaterialslett.4c02674>
26. Dagdelen, J., Dunn, A., Lee, S. *et al.* Structured information extraction from scientific text with large language models. *Nat Commun* **15**, 1418 (2024). <https://doi.org/10.1038/s41467-024-45563-x>
27. Polak, M.P., Morgan, D. Extracting accurate materials data from research papers with conversational language models and prompt engineering. *Nat. Commun.* **15**, 1569 (2024). <https://doi.org/10.1038/s41467-024-45914-8>

28. Schilling-Wilhelmi, M., Ríos-García, M., Shabih, S. et al. From text to insight: large language models for chemical data extraction. *Chem. Soc. Rev.* **54**, 1125-1150 (2025). <https://doi.org/10.1039/D4CS00913D>
29. Shetty, P., Rajan, A.C., Kuenneth, C. et al. A general-purpose material property data extraction pipeline from large polymer corpora using natural language processing. *npj Comput Mater* **9**, 52 (2023). <https://doi.org/10.1038/s41524-023-01003-w>
30. Swain, M. C., Cole, J. M. ChemDataExtractor: A toolkit for automated extraction of chemical information from the scientific literature. *J. Chem. Inf. Model.* **56**, 1894-1904 (2016). <https://doi.org/10.1021/acs.jcim.6b00207>
31. Ye, Y., Ren, J., Wang, S. et al. Construction and Application of Materials Knowledge Graph in Multidisciplinary Materials Science via Large Language Model. In *Advances in Neural Information Processing Systems* **37**, 56878-56897 (2024). <https://bytez.com/docs/neurips/95920/paper>
32. McCusker, J. P., Keshan, N., Rashid, S., Deagen, M., Brinson, C. & McGuinness, D. L. NanoMine: A Knowledge Graph for Nanocomposite Materials Science. In *The Semantic Web - ISWC 2020* (eds Pan, J. Z., Tamma, V., d'Amato, C., Janowicz, K., Fu, B., Polleres, A., Seneviratne, O. & Kagal, L.) Vol. 12507, 144- 159 (Springer International Publishing, 2020). [https://doi.org/10.1007/978-3-030-62466-8\\_10](https://doi.org/10.1007/978-3-030-62466-8_10)
33. Garay-Ruiz, D., Bo, C. Chemical reaction network knowledge graphs: the OntoRXN ontology. *J. Cheminform.* **14**, 29 (2022). <https://doi.org/10.1186/s13321-022-00610-x>
34. Venugopal, V., Olivetti, E. MatKG: An autonomously generated knowledge graph in Material Science. *Sci. Data* **11**, 217 (2024). <https://doi.org/10.1038/s41597-024-03039-z>
35. Nie, Z., Zheng, S., Liu, Y. et al. Automating materials exploration with a semantic knowledge graph for Li-ion battery cathodes. *Adv. Funct. Mater.* **32**, 2201437 (2022). <https://doi.org/10.1002/adfm.202201437>
36. Rydholm, E., Bastys, T., Svensson, E. et al. Expanding the chemical space using a chemical reaction knowledge graph. *Digital Discovery* **3**, 1378-1388 (2024). <https://doi.org/10.1039/D3DD00230F>
37. Statt, M. J., Rohr, B. A., Guevarra, D. et al. The materials experiment knowledge graph. *Digital Discovery* **2**, 909-914 (2023). <https://doi.org/10.1039/D3DD00067B>
38. M. Bran, A., Cox, S., Schilter, O. et al. Augmenting large language models with chemistry tools. *Nat. Mach. Intell.* **6**, 525-535 (2024). <https://doi.org/10.1038/s42256-024-00832-8>
39. Boiko, D. A.; MacKnight, R.; Kline, B.; Gomes, G. Autonomous Chemical Research with Large Language Models. *Nature* **624**, 570-578 (2023) <https://doi.org/10.1038/s41586-023-06792-0>

40. Ramos, M. C., Collison, C. J., White, A. D. A review of large language models and autonomous agents in chemistry. *Chem. Sci.* **16**, 2514-2572 (2025). <https://doi.org/10.1039/D4SC03921A>
41. Skarlinski, M. D., Cox, S., Laurent, J. M. et al. Language agents achieve superhuman synthesis of scientific knowledge. arXiv:2409.13740 (2024). <https://doi.org/10.48550/arXiv.2409.13740>
42. Chiang, Y., Hsieh, E., Chou, C.-H. et al. LLaMP: Large Language Model Made Powerful for High-fidelity Materials Knowledge Retrieval and Distillation. arXiv:2401.17244 (2024). <https://doi.org/10.48550/arXiv.2401.17244>
43. Yang, Z., Liu, W., Gao, B. et al. MOOSE-Chem: Large language models for rediscovering unseen chemistry scientific hypotheses. arXiv:2410.07076 (2025). <https://arxiv.org/abs/2410.07076>
44. Zhang, H., Song, Y., Hou, Z. et al. HoneyComb: A flexible LLM-based agent system for materials science. arXiv:2409.00135 (2024). <https://arxiv.org/abs/2409.00135>
45. Ghafarollahi, A. & Buehler, M. J. AtomAgents: Alloy design and discovery through physics-aware multi-modal multi-agent artificial intelligence. arXiv: 2407.10022 (2024). <https://arxiv.org/abs/2407.10022>
46. Szymanski, N.J., Rendy, B., Fei, Y. et al. An autonomous laboratory for the accelerated synthesis of novel materials. *Nature* **624**, 86-91 (2023). <https://doi.org/10.1038/s41586-023-06734-w>
47. Ferber, D., El Nahhas, O.S.M., Wölflein, G. et al. Development and validation of an autonomous artificial intelligence agent for clinical decision-making in oncology. *Nat. Cancer* **6**, 1337-1349 (2025). <https://doi.org/10.1038/s43018-025-00991-6>
48. Wei, J., Wang, X., Schuurmans, D., et al. Chain-of-thought prompting elicits reasoning in large language models. *Adv. Neural Inf. Process. Syst.* **35**, 24824-24837 (2022). [https://proceedings.neurips.cc/paper\\_files/paper/2022/file/9d5609613524ecf4f15af0f7b31abca4-Paper-Conference.pdf](https://proceedings.neurips.cc/paper_files/paper/2022/file/9d5609613524ecf4f15af0f7b31abca4-Paper-Conference.pdf)
49. Lewis, P., Perez, E., Piktus, A. et al. Retrieval-augmented generation for knowledge-intensive NLP tasks. In *Advances in Neural Information Processing Systems* (eds. H. Larochelle et al.) (NeurIPS, 2020). <https://doi.org/10.5555/3495724.3496517>
50. Liu, N. F., Lin, K., Hewitt, J. et al. Lost in the middle: how language models use long contexts. arXiv:2307.03172 (2023). <https://doi.org/10.48550/arXiv.2307.03172>
51. Ayala, O., Bechard, P. Reducing hallucination in structured outputs via Retrieval-Augmented Generation. In *Proceedings of the 2024 Conference of the North American Chapter of the Association for Computational Linguistics: Human Language Technologies (Volume 6: Industry Track)* (eds. Yang, Y., Davani, A., Sil, A. & Kumar, A.) 228-238 (Association for Computational Linguistics, 2024).

- <https://doi.org/10.18653/v1/2024.naacl-industry.19>
52. Maaten, L.; Hinton, G. Visualizing Data using t-SNE. *J. Mach. Learn. Res.* **9**(Nov), 2579-2605 (2008). [https://www.cns.nyu.edu/events/spf/SPF\\_papers/JMLR\\_Final.pdf](https://www.cns.nyu.edu/events/spf/SPF_papers/JMLR_Final.pdf)
  53. Blei, D. M., Ng, A. Y. & Jordan, M. I. Latent Dirichlet allocation. *J. Mach. Learn. Res.* **3**, 993-1022 (2003). <https://jmlr.csail.mit.edu/papers/v3/blei03a.html>
  54. Chen, J., Xiao, S., Zhang, P. et al. M3-Embedding: multi-linguality, multi-functionality, multi-granularity text embeddings through self-knowledge distillation. arXiv:2402.03216 (2025). <https://doi.org/10.48550/arXiv.2402.03216>
  55. Douze, M., Guzhva, A., Deng, C., et al. The Faiss library. arXiv:2401.08281 (2025). <https://doi.org/10.48550/arXiv.2401.08281>
  56. Yuan, Y., Liu, C., Yuan, J. et al. A hybrid RAG system with comprehensive enhancement on complex reasoning. arXiv: 2408.05141 (2024). <https://arxiv.org/abs/2408.05141>
  57. Han, H., Wang, Y., Shomer, H. et al. Retrieval-augmented generation with graphs (GraphRAG). arXiv: 2501.00309 (2025). <https://arxiv.org/abs/2501.00309>
  58. Prince, M.H., Chan, H., Vriza, A. et al. Opportunities for retrieval and tool augmented large language models in scientific facilities. *npj Comput Mater* **10**, 251 (2024). <https://doi.org/10.1038/s41524-024-01423-2>
  59. Gao, Y., Xiong, Y., Gao, X. et al. Retrieval-Augmented Generation for Large Language Models: A Survey. arXiv:2312.10997 (2024). <https://doi.org/10.48550/arXiv.2312.10997>
  60. Zhong, X., Jin, B., Ouyang, S. et al. Benchmarking retrieval-augmented generation for chemistry. arXiv:2505.07671 (2025). <https://arxiv.org/abs/2505.07671>
  61. Glass, M., Rossiello, G., Chowdhury, M. F. M. et al. Re2G: Retrieve, rerank, generate. In *Proceedings of the 2022 Conference of the North American Chapter of the Association for Computational Linguistics: Human Language Technologies* (eds. Carpuat, M., de Marneffe, M.-C. & Meza Ruiz, I. V.) 2701- 2715 (Association for Computational Linguistics, 2022). <https://doi.org/10.18653/v1/2022.naacl-main.194>
  62. Wellawatte, G. P., Guo, H., Lederbauer, M. et al. ChemLit-QA: a human evaluated dataset for chemistry RAG tasks. *Mach. Learn.: Sci. Technol.* **6**, 020601 (2025). <https://doi.org/10.1088/2632-2153/acxyz1>
  63. Yang, S., Gribovskaya, E., Kassner, N., et al. Do large language models latently perform multi-hop reasoning arXiv:2402.16837 (2025). <https://doi.org/10.48550/arXiv.2402.16837>
  64. Wu, L., Luo, N., Xie, Z., et al. Improved breakdown strength of Poly(vinylidene Fluoride)-based composites by using all ball-milled hexagonal boron nitride sheets without centrifugation. *Compos. Sci. Technol.* **190**, 108046 (2020).

<https://doi.org/10.1016/j.compscitech.2020.108046>

65. Tang, Y., Xu, W., Cao, J. et al. MatterChat: A multi-modal LLM for material science. *arXiv*: 2502.13107 (2025). <https://arxiv.org/abs/2502.13107>
66. Yu, Y., Wang, H., Zong, L., et al. ChatMolData: A Multimodal Agent for Automatic Molecular Data Processing. *Adv. Intell. Syst.*, **7**: 2401089 (2025). <https://doi.org/10.1002/aisy.202401089>
67. Li, J., Zhang, D., Wang, X., et al. ChemVLM: exploring the power of multimodal large language models in chemistry area. *arXiv*:2408.07246 (2025). <https://doi.org/10.48550/arXiv.2408.07246>